The Numerical Analysis of the Nonlinear Motion of a Flexible Rotating Beam

Fathy A. Elnaggar
Lecturer Assistant
Email: fathyf3@yahoo.com

Hanaa M. El-Absy
Lecturer
email: paper_fathy@yahoo.com

Galal A. Elkobrosy
Professor
Email: paper_fathy@yahoo.com

Mathematical Engineering Department - Faculty of Engineering
Alexandria University, Egypt. P.O.Box 21544

Abstract: The main objective of this work is to investigate the chaotic behavior motion of a dynamic model consisting of a flexible rotating beam with a constant angular velocity, $\dot{\theta}$, about the ***Z***-axis. This dynamic model is based on a beam with an isotropic material and a geometric nonlinear deformation. A continuous system is considered in the analysis-approach. Both of the in-plane and the out-of-plane transverse deformations are included. They are also represented by the mode shape function of the beam. Thus, the dynamic model is defined by ordinary differential equations with two degrees of freedom (2^{nd}***.D.F***). The governing differential equations are two coupled Duffing's equations. Dynamic numerical simulation methods are used to obtain the time history, phase portrait, Laypunov exponent, power spectrum, Poincare' maps and their fractal dimensions.

Key words: Nonlinear dynamics, chaos, and strange attractors.

1-Introduction:

It is well known that a dynamical system with nonlinear governing equations may exhibit a chaotic response at a certain combination of the excitation amplitudes and the system parameters. Over the past three decades, a numerous amount of theoretical calculations, simulations and experiments have been investigated on various nonlinear systems. This is in order to understand chaos and routes to chaos in such systems [1-6]. The dynamics of the rotating beam was the subject of many investigations [7-10]. The dynamics of a rotating structure is governed by a set of nonlinear differential equations, which exhibit a strong coupling between the reference displacement and the elastic deformations. The nonlinear inertia coupling between the rigid body and the elastic displacement manifests itself strongly in problems where mechanical systems are made of lightweight components and operate at a relatively high speed. EL-Absy and Shabana [21], developed a dynamic model for an Euler-Bernoulli rotating beam, and examined the nature of coupling between the rigid body and the elastic displacement. They examined the effect of the stability of the elastic modes on the stability of the rigid body motion of a rotating beam, analytically and numerically. Furthermore, they examined the effect of the geometric stiffness on the dynamic stability of a rotating beam. In this paper, the equations of motion (represented in the matrix form) of an Euler-Bernoulli rotating beam, subject to an external excitation force, are derived. This was achieved using both the Hamiltonian principle and the assumed mode method. Both the in-plane and the out-of-plane transverse deformations are included and they are represented by the mode shape function of the beam. When both the in-plane and the out-of plane transverse deformations are considered, the dynamic model is 2^{nd}***.D.F*** and the governing differential equations are two coupled Duffing's equations. Dynamic numerical simulation methods are used to obtain the time history, phase portrait, Laypunov exponent, power spectrum, Poincare' maps and their fractal dimensions.

2-Kinematics:

Figure (1}, shows ***O***, the origin of a set of mutually perpendicular axes ***OX, OY*** and ***OZ,*** which are fixed in an inertial reference frame. Another set of mutually perpendicular axes, ***Ox, Oy*** and ***Oz***, attached to one of the beam end points. This model consisted of a beam rotating with a constant angular velocity about the ***Z*-axis**. The global position vector of an arbitrary point ***P*** on the considered beam can be expressed by:

$$r_p = A\,\bar{r} \qquad (1)$$

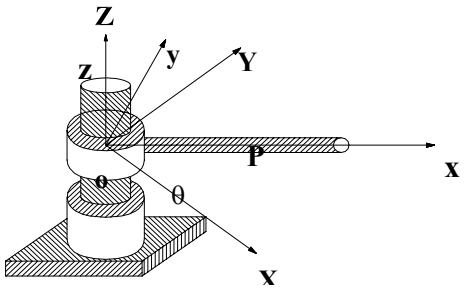

Figure 1: The Rotating Beam Model

where, $\bar{r}$ indicates the local position vector of the point, ***P***, in the deformed state (with respect to the fixed system-coordinates), and ***A*** indicates the transformation matrix, which defines the orientation of the body reference. The transformation matrix ***A*** is defined by:

$$A = \begin{bmatrix} cos\theta & -sin\theta & 0 \\ sin\theta & cos\theta & 0 \\ 0 & 0 & 1 \end{bmatrix} \qquad (2)$$

The position vector $\bar{r}$ can be written as:

$$\bar{r} = \bar{u}_0 + \bar{u}_f \quad (3)$$

where, the position vector of P, in the undeformed state $\bar{u}_0$, and the deformed position vector of P, with respect to the beam fixed coordinate $\bar{u}_f$, are represented by:

$$\bar{u}_0 = [x \quad 0 \quad 0] \quad (4)$$

$$\bar{u}_f = \begin{Bmatrix} \bar{u} \\ \bar{v} \\ \bar{w} \end{Bmatrix} = \begin{bmatrix} 0 & 0 \\ S_2 & 0 \\ 0 & S_3 \end{bmatrix} \begin{Bmatrix} q_2 \\ q_3 \end{Bmatrix} = [S]\{q_f\} \quad (5)$$

where, $\bar{u}$, $\bar{v}$ and $\bar{w}$ are the axial, in-plane and out-of-plane deformations with respect to the xyz coordinates, respectively, and q_2 and q_3 are the time dependent elastic generalized coordinates of the deformable beam. The overall generalized coordinates of the beam can be expressed as follows:

$$q = \left\{ \theta \quad \{q_f\}^T \right\}^T \quad (6)$$

where θ is defined as the rigid angular displacement. The velocity of P can be obtained by differentiating equation (3) with respect to time, so that:

$$\dot{r}_p = L_v \{\dot{q}\}^T \quad (7)$$

where, $\{\dot{q}\}^T$ is the generalized velocity of the beam and L_v is defined as:

$$L_v = [B \quad AS] \quad (8)$$

in which:

$$\mathbf{B} = \begin{bmatrix} -\sin\theta & -\cos\theta & 0 \\ \cos\theta & -\sin\theta & 0 \\ 0 & 0 & 0 \end{bmatrix} . \bar{\mathbf{r}} \quad (9)$$

3-Kinetic Energy: The kinetic energy of the beam is given by:

$$T = \frac{1}{2} \rho \int \dot{r}_p^T \dot{r}_p dV \quad (10)$$

where, ρ is defined as the constant mass density and $\dot{r}_p$ is the global velocity of any arbitrary point P on the beam. Substituting equation (7) into equation (10) yields to:

$$T = \frac{1}{2} \dot{q}^T M \dot{q} \quad (11)$$

in which:

$$M = \begin{bmatrix} m_{\theta\theta} & m_{\theta f} \\ m_{\theta f} & m_{ff} \end{bmatrix} \quad (12)$$

where,

$$\mathbf{m}_{\theta\theta} = \rho \int \mathbf{B}^T \mathbf{B} dV$$

$$\mathbf{m}_{\theta f} = \rho \int \mathbf{B}^T \mathbf{A} \mathbf{S} dV \quad (13)$$

$$\mathbf{m}_{ff} = \rho \int \mathbf{S}^T \mathbf{S} dV$$

In this case, the vectors q_2 and q_3 are reduced to scalars:

$$q_2 = q_2 \qquad q_3 = q_3 \quad (14)$$

Also, the following shape function matrix describes the deformation of the beam:

$$S = \begin{bmatrix} 0 & 0 \\ 3\xi^2 - \xi^3 & 0 \\ 0 & 3\xi^2 - \xi^3 \end{bmatrix} \quad (15)$$

The components $m_{\theta\theta}$, $m_{\theta f}$, and m_{ff} of the mass matrix are defined as:

$$m_{\theta\theta} = \frac{1}{3} m l^2 + \frac{33}{35} m q_2^2$$

$$m_{\theta f} = \frac{11}{20} m l [1 \quad 0]$$

$$m_{ff} = \frac{33}{35} m \begin{bmatrix} 1 & 0 \\ 0 & 1 \end{bmatrix}.$$

In terms of the components of the mass matrix, the kinetic energy of the beam can be written in the following form:

$$\mathbf{T} = \frac{1}{2} (\dot{\theta}^T \mathbf{m}_{\theta\theta} \dot{\theta} + 2\dot{\theta}^T \mathbf{m}_{\theta f} \dot{q}_f + \dot{q}_f^T \mathbf{m}_{ff} \dot{q}_f) \quad (16)$$

4-Strain Energy

The strain energy is not given by the same expression for the linear deformation and the geometric nonlinear case. For the linear deformation, the quadratic terms in the strain displacement relationship are neglected. However, the quadratic terms have to be retained in considering geometric nonlinearity. In this work, the nonlinear strain displacement is considered. Thus, the strain energy of the elastic beam is given by:

$$U = \frac{1}{2} \int \varepsilon_x \sigma_x dV \quad (17)$$

For an isotropic material

$$\sigma_x = E \varepsilon_x \quad (18)$$

where, E is the modulus of elasticity, σ_x is the normal stress and ε_x is the strain. Substituting equation (18}) into equation (17) yields to:

$$U = \frac{1}{2} \int E \varepsilon_x^2 dV \quad (19)$$

Using a nonlinear strain displacement relation including the quadratic terms, the normal strain can be written as:

$$\varepsilon_x = \frac{\partial u}{\partial x} - y\left(\frac{\partial^2 v}{\partial x^2}\right) - z\left(\frac{\partial^2 w}{\partial x^2}\right) + \frac{1}{2}\left(\frac{\partial v}{\partial x}\right)^2 + \frac{1}{2}\left(\frac{\partial w}{\partial x}\right)^2 \quad (20)$$

Using the shape matrix function defined by equation (15), the above equation can be written in the following form:

$$\mathbf{U} = \frac{\mathbf{6EI1}}{\mathbf{l^3}} * \left(q_2^2 + q_3^2 \right) + \frac{\mathbf{144}}{\mathbf{35}} \frac{\mathbf{EA}}{\mathbf{l^3}} \left(q_2^4 + q_3^4 \right) + \frac{\mathbf{288}}{\mathbf{35}} \frac{\mathbf{EA}}{\mathbf{l^3}} \left(q_2^2 * q_3^2 \right) \quad (21)$$

5-Evolution Equations: The equations of motion can be obtained by using Lagrange's formulation as follows:

$$\frac{d}{dt}\left(\frac{\partial T}{\partial \dot{q}} \right)^T - \left(\frac{\partial T}{\partial q} \right) + \left(\frac{\partial U}{\partial q} \right) = F_e \quad (22)$$

where, T is the kinetic energy, U is the strain energy and F_e is the generalized external force vector associated with the generalized coordinates. By performing the operation indicated in equation (22), the equations of motion can be represented in the following matrix form:

$$\mathbf{M_1}\ddot{q}_f + \left(\mathbf{K_{ff}} + \mathbf{K_G} + \mathbf{K_H}\right) q_f - \dot{\theta}^2 \mathbf{L}\, q_f - \dot{\theta}\, \mathbf{L_1}\, \dot{q}_f = \mathbf{F_e} \quad (23)$$

$$\mathbf{F_e} = -\mathbf{c}\, \dot{q}_f + \begin{bmatrix} \mathbf{f_1}\cos(\omega t) \\ \mathbf{f_2}\sin(\omega t) \end{bmatrix} \quad (24)$$

6-Numerical Results and Discussions: Direct numerical integration of the equation of motion is always an attractive option in finding the solution of nonlinear differential equation. The very remarkable algorithms to obtain time history, phase portrait, Lyapunov exponent, power spectrum, Poincare' maps and fractal dimension have been developed by Parker et al [22]. In this paper, equations (23) have been simulated using the fifth and the sixth order Runge Kutta Verner algorithm. The analysis started by considering both of the in-plane and the out-of-plane transverse deformations. The dynamical model is a 2nd. D.F., and the governing differential equations are two coupler Duffing's equations. The effect of varying the angular velocity, the amplitude of the excitation force and the damping coefficient were studied in detail. In the following analysis, a flexible beam of length l = 0.5 m, mass density ρ = 7800 kg/m^3, modules of elasticity E = 2* 10^{11} N/m^2 and area moment of inertia I were considered. The beam is assumed to have a circular cross section of diameter d = 0.01 m. The effect of the gravitational force is neglected and ω is considered to be $\omega = 1.0$. The analysis of this model takes a lot of time and effort to know the routes of chaos. Hence, to reach this aim and the time analysis, all parameters are fixed except one was varied until the chaotic response occurred. Then another parameter is varied while the others kept fixed and so on.

The first set of parameters was as follows; the amplitude of the excitation force, f_1, varies from **0** to **100**; the amplitude of the excitation force, $f_2 = 0$; the damping coefficient, c = **0.1**; the angular velocity, $\dot{\theta}$ = **100** rad/sec; and the initial conditions, $x_1 = 1$, $\dot{x}_1 = 0$, $x_2 = 1$ $\dot{x}_2 = 0$. When f_1 was increased, a small periodic motion appeared about the stable fixed point. By increasing its amplitude, the amplitude of the periodic motion increased until a sequence of period doubling bifurcation occurred. Further increase of f_1 led to a chaotic behavior with strange attractors in the (x_1 , $\dot{x}_1$) plane, but only led to fuzzy attractors in the (x_2 , $\dot{x}_2$) plane. Hence, the damping coefficient had to be increased in order to achieve strange attractors in both planes, as shown in figures (2,3).

The Second set of parameters used in analyzing this system was the same as that used for the first set with $\dot{\theta}$ = **350** rad/sec. The results obtained for the second set were similar to those obtained for the first one, but both of the period doubling bifurcation and the occurrence of strange attractors were existed at lower value of f1, as shown in figures (4,5,6). The third set of parameters used in analyzing this system was the same as that used for the above two sets, with $\dot{\theta}$ = **550** rad/sec. The results obtained for this set were similar to those obtained for both of the above two sets, but both of the period doubling bifurcation and the occurrence of strange attractors were existed at a much lower value of f1, as shown in figures (7,8,9).

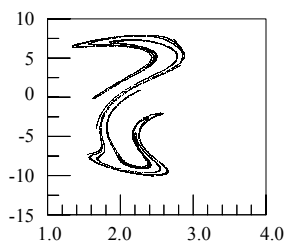

(a)

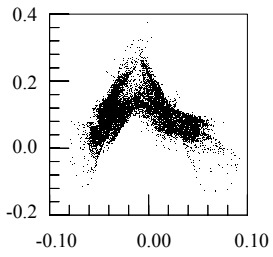

(b)

Figure 2: Poincare' maps indicating chaotic behavior at $\dot{\theta}$ = **100 rad/sec, f_2 = 0.0, c = 0.11, f_1 = 27** (a) Poincare' section x_1 , $\dot{x}_1$ (b) Poincare' section x_2 , $\dot{x}_2$

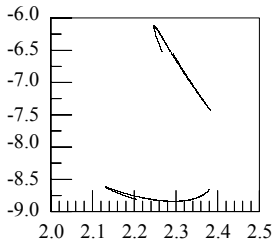

(a)

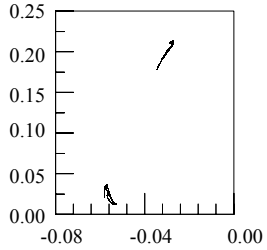

(b)

Figure 3: Poincare' maps indicating chaotic behavior at $\dot{\theta}$ **= 100 rad/sec, f_2 = 0.0, c = 0.11, f_1 = 27** (a) Poincare' section x_1 **,** $\dot{x}_1$ (b) Poincare' section x_2 **,** $\dot{x}_2$

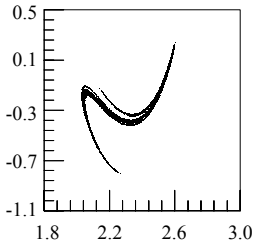

(a)

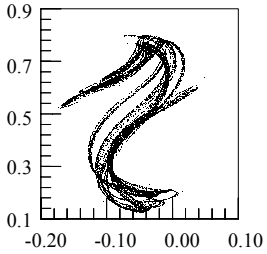

(b)

Figure 4:Poincare' maps indicating chaotic behavior at $\dot{\theta}$ **= 350 rad/sec f_2 = 0.0, c = 0.13,f_1 = 6.5** (a) Poincare' section x_1 **,** $\dot{x}_1$ (b) Poincare' section x_2 **,** $\dot{x}_2$

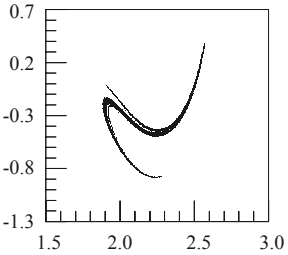

(a)

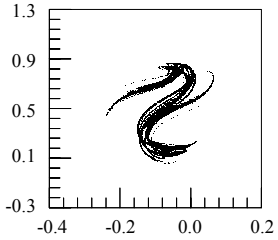

(b)

Figure 5: Poincare' maps indicating chaotic behavior at $\dot{\theta}$ **= 350 rad/sec f_2 = 0.0, c = 0.175, f_1 = 7.5** (a) Poincare' section x_1 **,** $\dot{x}_1$ (b) Poincare' section x_2 **,** $\dot{x}_2$

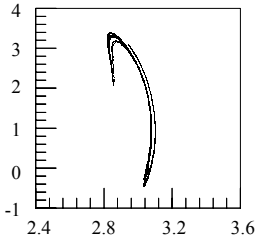

(a)

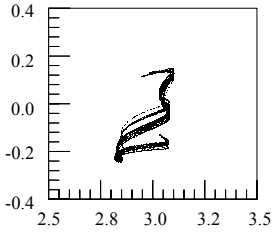

(b)

Figure 6: Poincare' maps indicating chaotic behavior at $\dot{\theta}$ **= 350 rad/sec f_2 = 0.0, c = 0.109, f_1 = 10** (a) Poincare' section x_1 **,** $\dot{x}_1$ (b) Poincare' section x_2 **,** $\dot{x}_2$

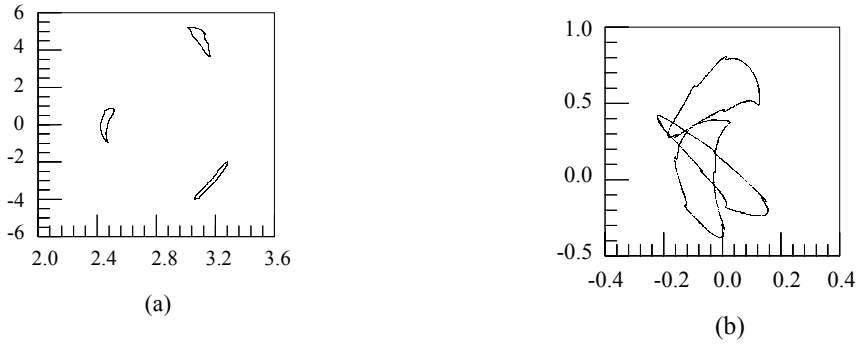

Figure 7: Poincare' maps indicating chaotic behavior at $\dot{\theta}$ **= 550 rad/sec f_2 = 0.0, c = 0.1, f_1 = 2.5** (a) Poincare' section x_1 , $\dot{x}_1$ (b) Poincare' section x_2 , $\dot{x}_2$

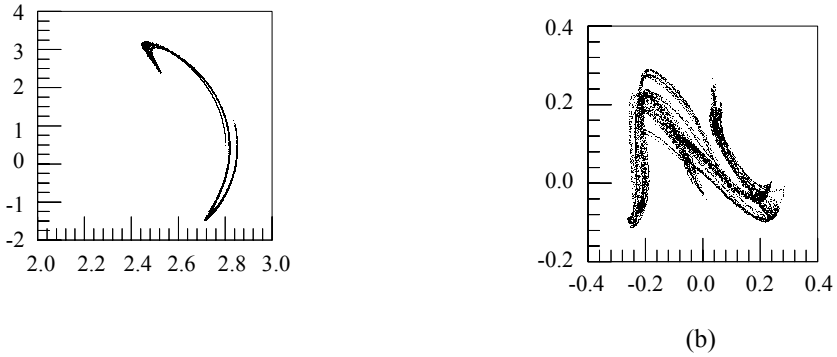

Figure 8: Poincare' maps indicating chaotic behavior at $\dot{\theta}$ **= 550 rad/sec f_2 = 0.0, c = 0.1, f_1 = 5.5** (a) Poincare' section x_1 , $\dot{x}_1$ (b) Poincare' section x_2 , $\dot{x}_2$

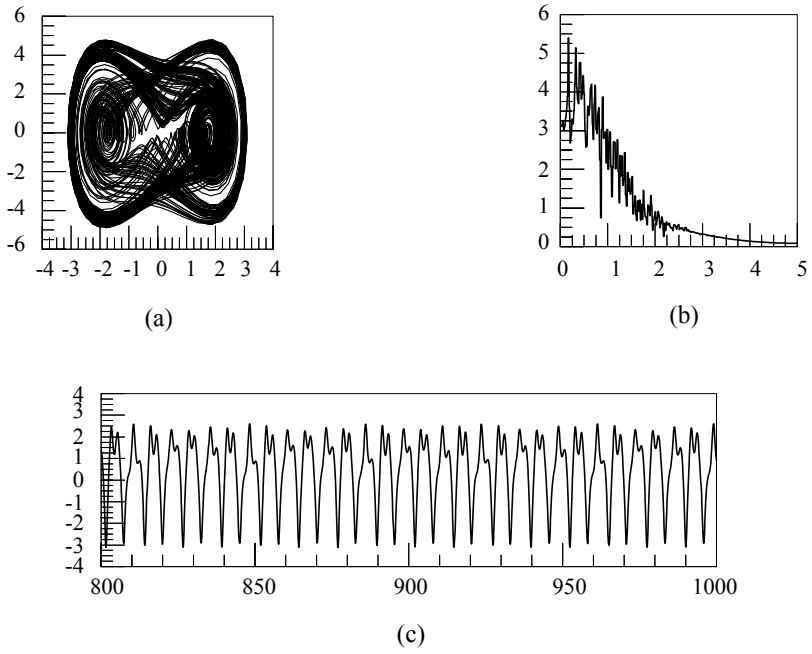

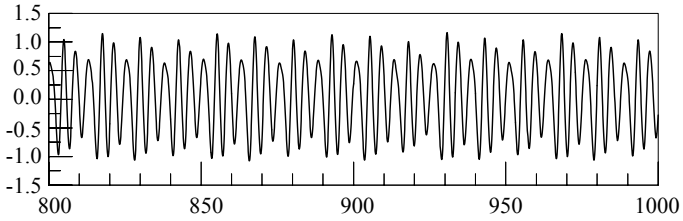

(d)

Figure 9: (a) Phase portrait (b) Power spectrum (c) Time history indicating chaotic behavior at $\dot{\theta}$ **= 550rad/sec f_2 = 0.0, c = 0.1, f_1 = 5.5**

7-Conclusion: The aim of this study was to investigate the chaotic behavior motion of a flexible rotating beam with constant angular velocity, about the ***Z***-axis. The beam considered was made of an isotropic material and had a geometrical nonlinear deformation. The in-plane and out-of-plane transverse deformations were represented by the mode shape function of the beam. This resulted in having two coupled Duffing's equations representing the motion of the beam. A study of this system was carried out for different values of its parameters. The results showed that, both the regular periodic solution and the chaotic behavior of the free-end of the rotating beam occurred at a certain combination of the system parameters. An interesting feature of this model (as shown by the numerical analysis) was the occurrence of a sequence of period doubling bifurcation, followed by chaotic behavior, at low values of the amplitude of the excitation force and high values of the angular velocity. Due to the very high simulation time that was required to run the coupled Duffing's equations, a more simplified model (obtained using only the in-plane deformation), which involved one Duffing's equation with one degree of freedom, was simulated. The numerical results obtained form this simplified model showed the existence of regular and chaotic motion, very similar to that obtained from the original system, but only occurring at slightly higher values of system parameters.

Reference

[1] Lorenz E.N. "Deterministic non-periodic flow". J. of the Atmosheric Sciences, 20(2):130-141, March 1963.

[2] Wolfe A., Swift J.L., Swinney H.L., and Vastano J. A. "Determine Lyapunov exponents from a time series". Physica 16D, pages 285-317, 1985.

[3] Rand R.H. and Holmes P.J. "Bifurcation of periodic motions in two weakly coupled Van der pol oscillators". J. Non-linear Mechanics, 15:387-399, 1980.

[4] Hirsch M.W. "The dynamical systems approach to differential equations". Bulletin (New Series) of the American Mathematical Society, 11(1): 1-64, July 1984.

[5] Henon M. "On the numerical computation of Poincarè maps". Physica 5D, Pages 412-414, 1982.

[6] Ditto W.L., Spano M.L. and Lindner J.F. "Techniques for the control of chaos". Physica D, 86:198-211, 1995.

[7] Liu X.Q. and Riggs H.S. "Vibration of free-free beam under tensile axial loads". Journal of sound and vibration, 190(2): 273-282, 1996

[8] Simo J.C. and Vu-Quoc L. "On the dynamics of flexible beam under large overall- the plane case, Part-I and Part-II". ASME Journal of applied Mechanics, 53:849-863, 1986.

[9] Belytschro T., Schwer L. and Klein M.J. "Large displacement, transient analysis of space frames". International Journal for Numerical Methods in Engineering, 11:65-84, 1977.

[10] Schreyer H.L. "Consistent diagonal mass matrices and finite element equations for one-dimensional problems". International Journal for Numerical Methods in Engineering, 12:1171-1184, 1978.

[11] H.El-Absy and A.A.Shabana "Coupling between rigid body and deformation modes". Journal of Sound and Vibration, 198(5):617-637, 1996.

[12] T.S.Parker and L.O.Chua. "Practical Numerical Algorithms for chaotic systems". Springer-Verlag, New York NY, 1980.